Agelas *Wasting Syndrome Alters Prokaryotic Symbiont Communities of the Caribbean Brown Tube Sponge,* Agelas tubulata

Lindsey K. Deignan, Joseph R. Pawlik & Patrick M. Erwin

Microbial Ecology

ISSN 0095-3628
Volume 76
Number 2

Microb Ecol (2018) 76:459-466
DOI 10.1007/s00248-017-1135-3

Springer

Microbial Ecology (2018) 76:459–466
https://doi.org/10.1007/s00248-017-1135-3

INVERTEBRATE MICROBIOLOGY

Agelas Wasting Syndrome Alters Prokaryotic Symbiont Communities of the Caribbean Brown Tube Sponge, *Agelas tubulata*

Lindsey K. Deignan[1] · Joseph R. Pawlik[1] · Patrick M. Erwin[1]

Received: 3 August 2017 / Accepted: 19 December 2017 / Published online: 3 January 2018

Abstract

The brown tube sponge *Agelas tubulata* (cf. *Agelas conifera*) is an abundant and long-lived sponge on Caribbean reefs. Recently, a disease-like condition, *Agelas* wasting syndrome (AWS), was described from *A. tubulata* in the Florida Keys, where prevalence of the syndrome increased from 7 to 35% of the sponge population between 2010 and 2015. In this study, we characterized the prokaryotic symbiont community of *A. tubulata* for the first time from individuals collected within the same monitoring plots where AWS was described. We also sampled tissue from *A. tubulata* exhibiting symptoms of AWS to determine its effect on the diversity and structure of prokaryotic symbiont communities. Bacteria from the phyla *Chloroflexi* and *Proteobacteria*, particularly the class *Gammaproteobacteria*, dominated the sponge microbiome in tissue samples of both healthy sponges and those exhibiting AWS. Prokaryotic community structure differed significantly between the diseased and healthy sponge samples, with greater variability among communities in diseased samples compared to healthy samples. These differences in prokaryotic community structure included a shift in relative abundance of the dominant, ammonia-oxidizing (*Thaumarchaeota*) symbionts present in diseased and healthy sponge samples. Further research is required to determine the functional consequences of this shift in microbial community structure and the causal relationship of dysbiosis and sponge disease in *A. tubulata*.

Keywords Microbiome · Porifora · Disease · *Thaumarchaeota* · Dysbiosis

Introduction

Sponges (Phylum Porifera) host diverse and abundant microbial communities [1–4], which may constitute up to 8×10^9 microbial cells/ml of sponge tissue [5]. Prokaryotic symbionts participate in a number of functions within the sponge, including nutrient cycling, the production of secondary metabolites, disease prevention, and antimicrobial and antifouling activity [1–3, 6]. However, the role of the microbiome within the sponge holobiont is not fully understood. Advancements in high throughput sequencing technology have made it easier to examine not just the structure of abundant microbial symbionts present in a sponge but also rare microbial species (e.g., deep amplicon sequencing) and functional characteristics (e.g., metatranscriptomics), thereby enhancing our ability to explore sponge microbiomes.

As marine sponges are becoming the focus of more research, reports of diseases affecting sponges are also increasing [7–14]. Despite the prevalence of sponge diseases, only two studies have successfully identified the etiological agents responsible for a sponge disease [13, 15]. In the Great Barrier Reef sponge *Rhopaloeides odorabile*, skeletal infections of spongin boring necrosis were caused by a novel strain of the alphaproteobacterium, *Pseudoalteromonas agarivorans* [15, 16]. Sweet et al. [13] found the cause of a disease affecting the sponge *Callyspongia* (*euplacella*) aff. *biru* in the Maldives to be the result of a consortium of a bacterium and a fungus. More frequently, studies have demonstrated shifts in the microbial communities of sponges as a result of, or initiating, the onset of disease infection [17–19]. Given the vast number of microbes associated not only with marine sponges but also present in the seawater, identifying the causative agent of a disease is often not possible. More recently, the view of pathogenesis has expanded away from a model of one microbe causing a disease to a "pathobiome" model, where the resulting disease-state is the product of shifting microbial

✉ Patrick M. Erwin
erwinp@uncw.edu

[1] Department of Biology and Marine Biology, Center for Marine Science, University of North Carolina Wilmington, 5600 Marvin K. Moss Lane, Wilmington, NC 28409, USA

symbiont communities in the face of biotic and abiotic stressors [20, 21].

The brown tube sponge *Agelas tubulata* (cf. *Agelas conifera*) is a common sponge on Caribbean coral reefs [14, 22]. Demographic analyses from the Florida Keys revealed the brown tube sponge to be abundant (mean density 0.30 ± 0.15 m^{-2}) with relatively stable populations [14]. *A. tubulata* is a slow-growing species that produces brominated pyrrole alkaloids as a chemical defense against predatory fishes [23–25]. Members of the genus *Agelas* have been categorized as high microbial abundance (HMA) sponges [25, 26]; however, until now, no comprehensive examination of the prokaryotic symbiont community of *A. tubulata* has been conducted [27].

Annual monitoring of populations of the brown tube sponge in survey plots on reefs in the Florida Keys led to the discovery of a condition known as *Agelas* wasting syndrome (AWS), which increased in prevalence from 7 to 35% of the population between 2010 and 2015 [14]. AWS is characterized by localized lesions that form from tissue necrosis, leading to shedding of the sponge skeleton. Sponges typically exhibited symptoms of AWS for multiple years, and while lesions could heal over time, tissue regrowth was slow for this slow-growing species [14]. The cause of AWS is currently unknown.

In this study, we characterized the prokaryotic symbiont community of *A. tubulata* from individuals collected within the same long-term monitoring plots in the Florida Keys where AWS was described [14]. We collected tissue samples from apparently healthy individuals and sponges exhibiting symptoms of AWS and compared the prokaryotic communities between the healthy and diseased sponges to investigate the pathobiome model of AWS infection in *A. tubulata*.

Materials and Methods

Sponge samples were collected at approximately 20-m depth from Conch Reef (24° 56′ 59″ N; 80° 27′ 13″ W) off Key Largo, Florida, USA, in June 2015. All sponges were part of a long-term monitoring program that included annual photography of each sponge from 2010 to 2015. Using the photographs, the severity of the disease was classified for each sponge annually. The percentage of sponge tissue affected by AWS was characterized using the following scale: 0 represented ≤ 1% affected tissue, 1 represented > 1–5% affected tissue, 2 represented 6–25% affected tissue, 3 represented 26–50% affected tissue, and 4 represented 51–100% affected tissue. Five sponges showing signs of AWS were sampled from within the diseased area (diseased), from the apparently healthy tissue (healthy), and from transitional tissue in contact with, but not part of, the diseased areas (transitional). AWS lesions are characterized by a lighter tissue color, and lesion growth occurs by the shedding of the sponge tissue leaving behind spongin fibers which slough away in time [14]. The diseased tissue samples collected were composed primarily of the lighter-colored sponge tissue, to focus the sampling on the sponge microbiome and avoid as much as possible opportunistic colonizers to the spongin fibers. All diseased samples were collected from sponges exhibiting symptoms of AWS for at least 3 years prior to sampling (Table 1). Additionally, tissue samples were taken from five sponges with no symptoms of AWS (control), and four ambient seawater samples (1 L each) were collected and concentrated on 0.2-μm filters. Samples were fixed in absolute ethanol and stored at −20 °C. DNA extraction was conducted using the DNeasy Tissue and Blood extraction kit (QIAGEN), following the protocol provided by the manufacturer. The bacterial/archaeal primers 515F and 806R [28] were used to amplify and sequence the V4 region of the 16S rRNA gene on an Illumina MiSeq platform at Molecular Research LP (Shallowater, TX).

A modified version of the Illumina MiSeq SOP pipeline [https://www.mothur.org/wiki/MiSeq_SOP] was used to process the raw sequence reads using mothur v 1.35.1 [29]. Briefly, low quality sequence reads were removed, and the remaining sequences were aligned and trimmed to the SILVA reference database (V4 region). Sequences that matched within two base pairs were pre-clustered [30] and putative chimeras were removed, as well as any non-targeted (chloroplast, mitochondria, eukarya) sequence reads. Operational taxonomic unit (OTUs) (97%) were formed using the average neighbor clustering algorithm and assigned consensus taxonomic names. Singletons (i.e., OTUs occurring once across the global dataset) were removed to avoid biasing diversity measures. Finally, the dataset was subsampled to the lowest number of sequence reads per sample ($n = 30{,}692$) to account for variation in sampling depths. Raw sequence data were deposited in the NCBI Sequence Read Archive under the accession numbers SAMN07125147-SAMN07125170.

Measures of alpha diversity were assessed for each sample group by calculating observed richness (number of unique OTUs), estimated richness (Chao estimator), evenness (Shannon), and diversity (inverse Simpson index) in mothur v 1.35.1. Analyses of variance (ANOVA) were conducted to test for differences in means among sample groups, and when significant, followed by post hoc Tukey's honest significant difference (HSD) tests to identify significantly different groups. ANOVA and Tukey's HSD were calculated in R v 3.3.1.

Prokaryotic community structure among groups (beta diversity) was examined using Bray-Curtis similarity matrices of square root transformed data and visualized in non-metric multidimensional scaling (nMDS) plots using PRIMER v 6.1.11. Seawater samples were excluded from the nMDS plot

Table 1 Annual disease classification of each sponge individual (three-letter code) sampled in this study, based on analysis of monitoring photographs

Category	Sponge	2010	2011	2013	2014	2015
Diseased	YZG	0	1	2	4	4
	YGM	0	1	4	4	4
	YHN	NA	0	3	4	3
	YWL	0	0	1	4	3
	YSB	0	0	1	2	3
Control	YYI	0	0	0	0	0
	YXZ	0	0	2	0	0
	YSI	0	0	0	0	0
	YSQ	0	0	0	0	0
	YGZ	NA	0	0	0	0

The percentage of sponge tissue affected by AWS is shown over a 5-year period using the following scale: 0 represented ≤ 1% affected tissue, 1 represented > 1–5% affected tissue, 2 represented 6–25% affected tissue, 3 represented 26–50% affected tissue, and 4 represented 51–100% affected tissue

NA not available

for better resolution of differences among sponge groups. Permutational multivariate ANOVA (PERMANOVA) were conducted to determine significant differences in community structure among groups using the PERMANOVA+ add-on in PRIMER. Finally, permutational multivariate analysis of dispersion (PERMDISP) were conducted to test for unequal dispersion of variability (i.e., distances from centroids in the nMDS plot) and interpret the differences detected by the PERMANOVA. For both the PERMANOVA and the PERMDISP analysis, multiple pairwise comparisons were corrected based on the Benjamini and Yekutieli (B-Y) false discovered rate control [31].

Two methods were used to examine the contribution of individual OTUs to community-level differences detected among sponge groups. Only sponge groups that showed significant differentiation based on the PERMANOVA analysis were included in OTU level analyses. The first analysis was Metastats [32], as implemented in mothur, which detects differentially abundant OTUs between groups based on their corrected relative abundance. Secondly, a similarity percentage (SIMPER) analysis was run in PRIMER, which quantifies the contribution of individual OTUs to overall dissimilarity between groups. To reduce the probability of false positive results from high numbers of pairwise comparisons, only abundant OTUs (> 1% relative abundance) were considered for Metastats analysis and only OTUs contributing > 0.5% to the dissimilarity between groups were considered in the SIMPER analysis. Representative sequences of OTUs that were found to contribute to differences between sample groups were analyzed using nucleotide-nucleotide BLAST search [33] to find the most closely related sequence.

Results

A total of 4767 unique OTUs were identified from all sample groups. The diseased group had the highest number of unique OTUs ($n = 2519$) and included representatives of 28 bacterial phyla and 61 bacterial classes. The control group (1678 unique OTUs) and transitional group (1726 unique OTUs) each hosted 23 bacterial phyla and 45 classes, and the healthy group had 1814 unique OTUs represented by 26 phyla and 53 classes. The seawater group had the lowest overall number of unique OTUs ($n = 1441$) and included representatives of 27 phyla and 51 classes. Symbiont OTUs affiliated with the phyla *Chloroflexi* and *Proteobacteria*, particularly class *Gammaproteobacteria*, dominated the sponge microbiomes, while class *Alphaproteobacteria* was the dominant bacterial taxon in seawater samples (Fig. 1).

Significant differences (ANOVA, $p < 0.05$) in the alpha diversity of prokaryotic communities in sponges and seawater were detected for the metrics richness, Chao richness, Shannon evenness, and inverse Simpson index. Tukey's HSD tests revealed that the differentiation was driven by the Seawater group, which exhibited significantly lower values for evenness and diversity compared to all sponge groups, and significantly lower richness (Chao) values compared to diseased and transitional sponge groups (Table 2). The mean observed richness of prokaryotic communities in the diseased group was significantly higher than other sponge groups, while the estimated (Chao) richness of the diseased group was between those calculated for the transitional and healthy groups. For both richness metrics, the standard deviation for the diseased samples was higher than that of the other groups, indicating greater variance in the number of OTUs per sample. All sponge groups had similarly even prokaryotic communities. The overall mean inverse Simpson index of the diseased samples was slightly higher than other sample groups; however, no significant differences occurred among sponge groups for this diversity measure.

In the nMDS plot based on prokaryotic community similarity, the healthy, control, and transitional sponge samples grouped together more closely than the diseased samples (Fig. 2). PERMANOVA analysis revealed significant differentiation in prokaryotic community structure between the seawater and all sponge groups and significant differentiation between the diseased and the control groups (Table 3). PERMDISP analysis confirmed higher dispersion (variability) among diseased sponge microbiomes compared to other sponge groups and similar dispersion among sponge microbiomes in transitional, healthy, and control groups.

SIMPER analyses comparing the prokaryotic communities from diseased and control sponges revealed that 13 OTUs individually contributed to ≥ 0.5% of the observed community level differences between microbiomes (Table 4). The single OTU with the greatest contribution to the dissimilarity between the

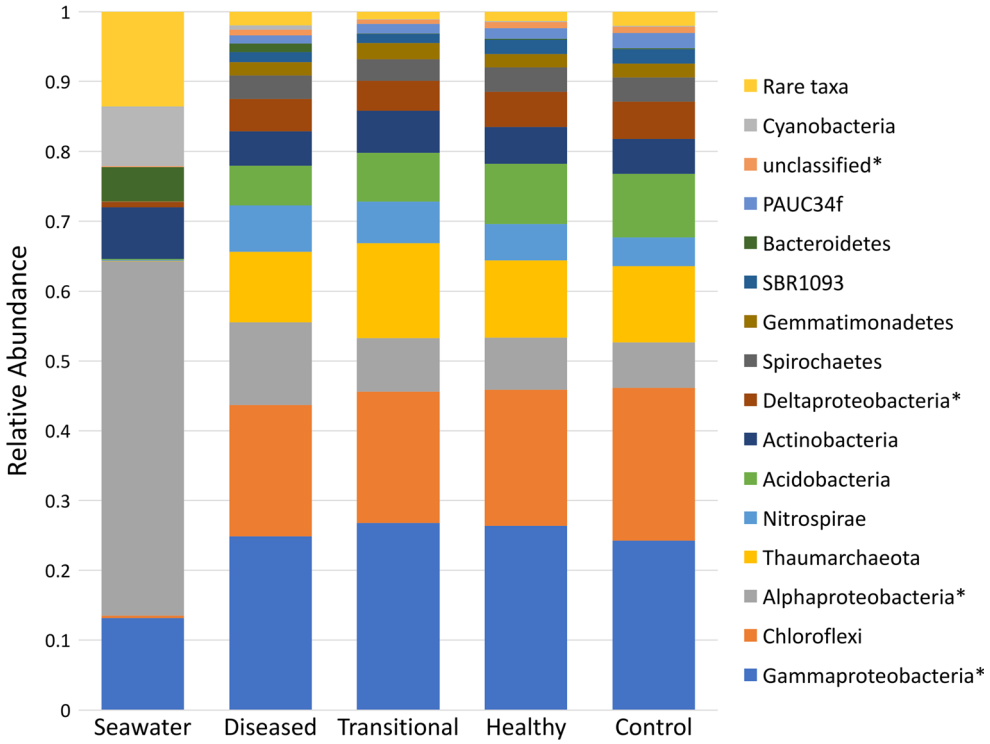

Fig. 1 Taxonomic composition of prokaryotic communities in *A. tubulata* and ambient seawater, showing mean abundance at the phylum level. Asterisks indicate class level within the phylum *Proteobacteria*

diseased and control sponges matched closely (99% sequence identity) to the archaeon *Cenarchaeum symbiosum* (OTU 6). This OTU exhibited significantly (Metastats) higher relative abundance in control compared to diseased sponges (Table 4). Interestingly, the most abundant OTU in diseased sponges identified by Metastats analysis also matched closely (99% sequence identity) to *C. symbiosum* (OTU 2). While both OTUs matched to the same archaeal species, they exhibited opposite relative abundance patterns, with OTU 2 exhibiting higher relative abundance in diseased compared to control sponges. Other important OTUs contributing to the differentiation of the diseased and control samples included members of the phyla *Proteobacteria*, *Acidobacteria*, and *Chloroflexi* (Table 4).

Discussion

Similar to previous studies of diseased sponges, we documented a shift in the prokaryotic community structure of sponges in response to disease [17–19, 34, 35]. Diseased individuals of *A. tubulata* had prokaryotic communities that were distinct from the control, healthy, and transitional samples. Additionally, the transitional samples were not distinct from the healthy and control samples, indicating that disruption of the sponge microbiome is confined to the AWS lesions and does not precede infection. AWS is not characterized by a visible transition zone separating healthy tissue from the disease lesions; our transitional samples were composed of sponge tissue that was in contact with disease lesions. In contrast, for the Mediterranean sponge *Ircinia fasciculata*, in which transitional tissue samples had significantly higher diversity as a result of more low-abundance OTUs than the healthy tissue, the transitional zone was characterized by noticeably lighter tissue coloration and decreased cyanobacterial abundance [19]. Overall, AWS resulted in general disruption of the resident microbiome in *A. tubulata*, with diseased samples exhibiting greater dissimilarity in symbiont structure compared to control, healthy, and transitional groups.

Table 2 Alpha diversity metrics for prokaryotic communities in *A. tubulata* and ambient seawater, showing observed OTU richness (Obs.), expected OTU richness (Chao), Shannon evenness, and inverse Simpson diversity values (± standard deviation) for each sample group

Group	Richness (Obs.)	Richness (Chao)	Evenness (Shannon)	Diversity (inv. Simpson)
Diseased	852 ± 169.48^	1650.58 ± 242.51^	0.61 ± 0.02^	30.85 ± 7.47^
Transitional	585 ± 27.11*	1694.91 ± 117.49 ^	0.60 ± 0.03^	25.71 ± 6.48^
Healthy	619.8 ± 52.67*	1586.17 ± 87.59^*	0.61 ± 0.01^	29.56 ± 2.62^
Control	575.2 ± 53.05*	1507.08 ± 187.65^*	0.61 ± 0.02^	27.70 ± 4.42^
Seawater	736.5 ± 22.87^*	1286.95 ± 60.81*	0.54 ± 0.01*	10.89 ± 0.83*

Different symbols represent significant pairwise comparisons ($P < 0.05$)

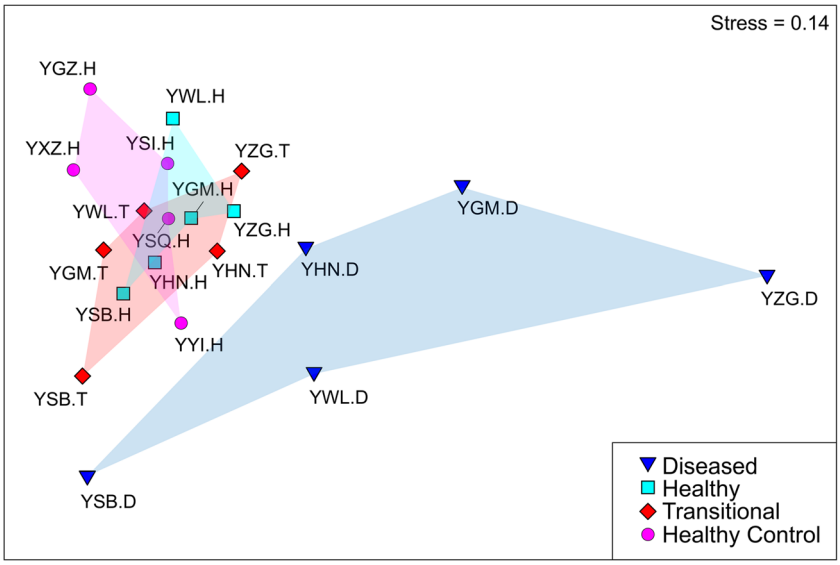

Fig. 2 nMDS plot of prokaryotic community structure in diseased (dark blue triangles), healthy (light blue squares), and transitional (red diamonds) tissue of AWS-affected individuals, and healthy control (pink circles) individuals of *A. tubulata* based on Bray-Curtis similarity. Labels denote sponge individuals

Interestingly, the two diseased sponge individuals that exhibited the greatest dissimilarity in microbiome structure compared to healthy individuals (sponges YZG and YGM) were also the two sponges with the greatest proportions of tissue affected by AWS (> 50%), and both displayed increasing disease lesions leading up to sampling (Table 1). In contrast, the remaining three diseased sponges exhibited microbiomes more similar to healthy individuals than the diseased individuals YZG and YGM, had lower proportions of affected tissue (< 50%), and, in some cases, had lesions that had been decreasing in size leading up to the time of sampling. This suggests that progressive degeneration of the microbiome occurs as the disease spreads, with some capacity for resilience until a dysbiosis threshold in sponge lesions is reached from which the sponges are unable to recover, consistent with the pathobiome model of disease onset [20, 21].

Table 3 Pairwise statistical comparisons of prokaryotic community structure (PERMANOVA) and dispersion (PERMDISP) in *A. tubulata* and ambient seawater. Italic *P* values indicate significant comparisons following Benjamini and Yekutieli (B-Y) corrections

	PERMANOVA		PERMDISP	
Pairwise comparison	*t*	*P*	*t*	*P*
Seawater, diseased	4.4998	*0.015*	11.468	*0.012*
Seawater, healthy	5.5304	*0.008*	12.353	*0.017*
Seawater, transitional	5.3624	*0.008*	14.010	*0.009*
Seawater, control	5.2418	*0.011*	8.9623	0.021
Diseased, healthy	1.2021	0.025	4.7166	*0.008*
Diseased, transitional	1.1583	0.083	3.8668	*0.011*
Diseased, control	1.3366	*0.005*	3.4162	*0.006*
Healthy, transitional	0.9283	0.816	1.2971	0.179
Healthy, control	0.9182	0.947	0.8829	0.408
Transitional, control	1.0723	0.157	0.0938	0.880

One significant difference between the diseased and control sponges was a shift in dominant symbiont taxa affiliated with *Thaumarchaeota*. In both the diseased and control sponges, two dominant *Thaumarchaeota* OTUs were present that exhibited high similarity (99% sequence identity) to previously described symbionts from *A. tubulata* [27]. OTU 2, which was significantly more abundant in diseased sponges, matched to three different archaeal sequences (ACEA3, ACAA13, ACEA1) detected in both adult sponges and embryos of *A. tubulata*, indicating vertical transmission [27]. OTU 6, which had a significantly lower abundance in diseased sponges, matched to an archaeal sequence (ACAA6) detected in adult *A. tubulata* [27]. Previous studies have also documented a shift in dominant *Thaumarchaeota* taxa between healthy and unhealthy sponges; López-Legentil et al. [34] found a shift in the *Thaumarchaeota* (formally *Crenarchaeota)* community in healthy and bleached specimens of the Caribbean giant barrel sponge, *Xestospongia muta*. Healthy *X. muta* were dominated by *Thaumarchaeota* that had previously been identified as sponge symbionts, while bleached *X. muta* were dominated by *Thaumarchaeota* associated with sediment. *Thaumarchaeota* are ammonia-oxidizing *Archaea* [36, 37], and in *X. muta*, the shift in the dominant *Thaumarchaeota* was accompanied by an increase in the expression of ammonia monooxygenase genes (*amoA*) in bleached sponges [34]. Both of the dominant *Thaumarchaeota* OTUs detected in *A. tubulata* herein matched to sponge symbionts, rather than taxa associated with environmental sources, as reported for *X. muta*. However, the observed shift in dominant *Thaumarchaeota* may contribute to a functional shift in the ammonia oxidation capacity of the sponge holobiont [34, 38, 39], with the disease lesions

Table 4 Microbial OTUs in *A. tubulata* that contributed at least 0.5% of the community dissimilarity (SIMPER analysis) between the diseased and control groups

OTU	Phylum	Lowest taxonomic classification	Relative Abundance (%)		Contribution to dissimilarity (%)
			Diseased	Control	
6*	*Thaumarchaeota*	*Cenarchaeum symbiosum*	1.7	6.0	1.12
21*	*Proteobacteria*	Order *Rhodobacterales*	1.8	0.5	0.79
1	*Proteobacteria*	Family *Ectothiorhodospiraceae*	7.2	8.9	0.72
2*	*Thaumarchaeota*	*Cenarchaeum symbiosum*	8.2	4.7	0.69
13	*Proteobacteria*	Order *Sphingomonadales*	3.9	1.9	0.65
12	*Chloroflexi*	Class SAR202	2.5	3.6	0.64
11*	*Acidobacteria*	Family PAUC26f	1.9	3.7	0.64
49	*Proteobacteria*	Family *Ectothiorhodospiraceae*	1.1	0.1	0.57
4	*Nitrospirae*	Family *Nitrospiraceae*	6.6	4.1	0.56
34	*Proteobacteria*	Class *Gammaproteobacteria*	1.0	0.8	0.54
5	*Chloroflexi*	Order TK18	4.0	5.6	0.54
38	*Proteobacteria*	Class *Alphaproteobacteria*	0.7	1.0	0.52
7	*Actinobacteria*	Phylum *Actinobacteria*	4.0	3.9	0.5
18*	SBR1093	Class EC214	1.4	2.1	< 0.5
15*	*Acidobacteria*	Order iii1–15	1.4	2.5	< 0.5

Phylum affiliation, lowest taxonomic classification, and average relative abundance in each sponge group are shown. Asterisks indicate OTUs exhibiting significantly different relative abundances between the diseased and control groups, according to metastats analysis

creating an improved environment for OTU 2 proliferation, perhaps due to an increase in the ammonia released by the necrotic sponge tissue.

In addition to the differential abundance of shared prokaryotic taxa, we also identified several bacterial OTUs that were present in the diseased sponges and absent in the healthy and control sponges: two *Proteobacteria* from the family *Rhodobacteraceae* (OTU 483 and OTU 279; relative abundances 0.01 and 0.03%, respectively), and a cyanobacterium from the order *Chroococcales* (OTU 457; relative abundance 0.01%). OTU 483 matched (100%) in BLAST to two environmental bacteria collected from biofilms examined in the Mediterranean Sea (JF948616) and on the Great Barrier Reef (HQ601712), indicating that the source of this bacterium is likely from the environment and may be a useful target for future studies on the spread of AWS. OTU 279 matched (99%) to four uncultured bacteria in BLAST, including two *Alphaproteobacteria* (accession numbers EF629653 and EF629647) from *Ircinia strobilina* collected from reefs off Key Largo, Florida. OTU 457 had a 98% sequence match to a bacterium from healthy tissue of the coral *Montastraea faveolata* (FJ203604), which underwent a similar pattern of increased microbial diversity in response to White Plague Disease [40]. However, OTU 457 also matched (98%) to a bacterium (HQ601736) from the same biofilm community on the Great Barrier Reef as OTU 483 [41]. The presence of particular bacteria in diseased individuals (and their absence in healthy individuals) is not sufficient to conclude that these bacteria contributed to disease infection, but provides specific targets for future examination of AWS amidst the vast diversity of sponge microbiomes. Indeed, the presence of these taxa in diseased sponges may result from opportunistic colonization of necrotic sponge tissue. For example, several previous studies identified specific bacteria or cyanobacteria that were only associated with diseased sponges, yet tissue transplantation experiments failed to induce infection [9, 12, 17].

In this study, we characterized the prokaryotic community of *A. tubulata* and the resulting microbiome shift in response to AWS infection. Healthy individuals were dominated by symbionts affiliated with *Chloroflexi*, *Proteobacteria*, and *Thaumarchaeota*, consistent with the categorization of *A. tubulata* as an HMA sponge and past studies on its microbiome [27, 42]. We further showed that AWS causes the prokaryotic community to differentiate from that of apparently healthy sponge tissue, and that changes to the sponge microbiome are confined to the disease lesions. Within the diseased samples, sponges with the most severe lesions had the highest prokaryotic diversity and showed the greatest differentiation from the remaining sponge samples, suggesting that the pathobiome may influence disease virulence. When focusing on specific OTUs that drove community-level differences between the control and diseased samples, we report a

structural shift in the dominant *Thaumarchaeota* taxa that may reflect a functional change in the ammonia-oxidizing capacity of the sponge holobiont. Future studies examining gene expression in control and diseased sponges are needed to elucidate the functional changes occurring in *A. tubulata* as a response to AWS. The impacts of AWS on sponge growth and reproduction have yet to be quantified, although it seems likely that the consequences are negative for both, resulting in reduced population growth for this species. Continued monitoring efforts are warranted to examine how shifts (or stability) in microbiome structure may allow some individuals to recover from AWS, while other sponges experience increased spread of AWS lesions, thereby providing key insights into the relationships between dysbiosis, disease progression, and host health.

Acknowledgements The authors thank the staff of the FIU's Aquarius Reef Base in Key Largo, Florida, for logistical support. Research in the Florida Keys National Marine Sanctuary was performed under permit FKNMS-2012-162.

Funding This study was funded by grants from the National Science Foundation, Biological Oceanography Program to J.R.P. (OCE-0095724, 0550468, 1029515), and to P.M.E. and J.R.P. (1558580).

Compliance with Ethical Standards

Conflict of Interest The authors declare that they have no competing interests.

References

1. Hill RT (2004) Microbes from marine sponges: a treasure trove of biodiversity for natural products discovery. In: Bull AT (ed) Microbial diversity and bioprospecting. ASM Press, Washington, DC, pp 177–190
2. Taylor MW, Radax R, Steger D, Wagner M (2007) Sponge-associated microorganisms: evolution, ecology, and biotechnological potential. Microbiol Mol Biol Rev 71:295–347
3. Webster NS, Taylor M (2012) Marine sponges and their microbial symbionts: love and other relationships. Environ Microbiol 14: 335–346
4. Thomas T, Moitinho-Silva L, Lurgi M, Björk JR, Easson C, Astudillo-García C, Olson JB, Erwin PM, Lopez-Legentil S, Luter H, Chaves-Fonnegra A, Costa R, Schupp PJ, Steindler L, Erpenbeck D, Gilbert J, Knight R, Ackermann G, Lopez JV, Taylor MW, Thacker RW, Montoya JM, Hentschel U, Webster NS (2016) Diversity, structure and convergent evolution of the global sponge microbiome. Nat Commun 7:11870
5. Webster NS, Hill RT (2001) The cultural microbial community of the great barrier reef sponge *Rhopaloeides odorabile* is dominated by an α-proteobacterium. Mar Biol 138:843–851
6. Thomas T, Rusch D, DeMaere MZ, Yung PY, Lewis M, Halpern A, Heidelberg KB, Egan S, Steinberg PD, Kjelleberg S (2010) Functional genomic signatures of sponge bacteria reveal unique and shared features of symbiosis. ISME J 4:1557–1567
7. Rützler K (1988) Mangrove sponge disease induced by cyanobacterial symbionts: failure of a primitive immune system? Dis Aquat Org 5:143–149
8. Cowart JD, Henkel TP, McMurray SE, Pawlik JR (2006) Sponge orange band (SOB): a pathogenic-like condition of the giant barrel sponge, *Xestospongia muta*. Coral Reefs 25:513–513
9. Olson JB, Gochfeld DJ, Slattery M (2006) *Aplysina* red band syndrome: a new threat to Caribbean sponges. Dis Aquat Org 71:163–168
10. Webster NS (2007) Sponge disease: a global threat? Environ Microbiol 9:1363–1375
11. Maldonado M, Sanchez-Tocino L, Navarro C (2010) Recurrent disease outbreaks in corneous demosponges of the genus *Ircinia*: epidemic incidence and defense mechanisms. Mar Biol 157:1577–1590
12. Angermeier H, Glöckner V, Pawlik JR, Lindquist NL, Hentschel U (2012) Sponge white patch disease affecting the Caribbean sponge *Amphimedon compressa*. Dis Aquat Org 99:95–102
13. Sweet M, Bulling M, Cerrano C (2015) A novel sponge disease caused by a consortium of micro-organisms. Coral Reefs 34:871–883
14. Deignan LK, Pawlik JR (2016) Demographics of the Caribbean brown tube sponge *Agelas tubulata* on Conch Reef, Florida Keys, and a description of *Agelas* wasting syndrome (AWS). Proc 13th ICRS, Honolulu, pp 72–4
15. Webster NS, Negri AP, Webb RI, Hill RT (2002) A spongin-boring α-proteobacterium is the etiological agent of disease in the great barrier reef sponge *Rhopaloeides odorabile*. Mar Ecol Prog Ser 232:305–309
16. Choudhury JD, Pramanik A, Webster NS, Llewellyn LE, Gachhui R, Mukherjee J (2015) The pathogen of the great barrier reef sponge *Rhopaloeides odorabile* a new strain of *Pseudoalteromonas agarivorans* containing abundant and diverse virulence-related genes. Mar Biotechnol 17:463–478
17. Angermeier H, Kamke J, Abdelmohsen U, Krohne G, Pawlik J, Lindquist N, Hentschel U (2011) The pathology of sponge orange band disease affecting the Caribbean barrel sponge *Xestospongia muta*. FEMS Microbiol Ecol 75:218–230
18. Olson JB, Thacker RW, Gochfeld DJ (2014) Molecular community profiling reveals impacts of time, space, and disease status on the bacterial community associated with the Caribbean sponge *Aplysina cauliformis*. FEMS Microbiol Ecol 87:268–279
19. Blanquer A, Uriz MJ, Cebrian E, Galand PE (2016) Snapshot of a bacterial microbiome shift during the early symptoms of a massive sponge die-off in the western Mediterranean. Front Microbiol 7. https://doi.org/10.3389/fmicb.2016.00752
20. Vayssier-Taussat M, Albina E, Citti C, Cosson J-F, Jacques M-A, Lebrun MH, Le Loir Y, Ogliastro M, Petit M-A, Roumagnac P, Candresse T (2014) Shifting the paradigm from pathogens to pathobiome: new concepts in the light of meta-omics. Front Cell Infect Microbiol 4:29. https://doi.org/10.3389/fcimb.2014.00029
21. Sweet M, Bulling M (2017) On the importance of the microbiome and pathobiome in coral health and disease. Front Mar Sci 4:9. https://doi.org/10.3389/fmars.2017.00009
22. Loh T-L, Pawlik JR (2014) Chemical defenses and resource trade-offs structure sponge communities on Caribbean coral reefs. Proc Natl Acad Sci USA 111:4151–4156
23. Pawlik JR, Chanas B, Toonen RJ, Fenical W (1995) Defenses of Caribbean sponges against predatory reef fish: I. Chemical deterrency. Mar Ecol Prog Ser 127:183–194
24. Assmann M, Lichte E, Pawlik JR, Köck M (2000) Chemical defenses of the Caribbean sponges *Agelas wiedenmayeri* and *Agelas conifera*. Mar Ecol Prog Ser 207:255–262
25. Richelle-Maurer E, De Kluijver MJ, Feio S, Gaudêncio S, Gaspar H, Gomez R, Tavares R, Van de Vyver G, Van Soest RWM (2003) Localization and ecological significance of oroidin and sceptrin in the Caribbean sponge *Agelas conifera*. Biochem Syst Ecol 31: 1073–1091

26. Gloeckner V, Wehrl M, Moitinho-Silva L, Gernert C, Schupp P, Pawlik JR, Lindquist NL, Erpenbeck D, Wörheide G, Hentschel U (2014) The HMA-LMA dichotomy revisited: an electron microscopical survey of 56 sponge species. Biol Bull 227:78–88
27. Schmitt S, Angermeier H, Schiller R, Lindquist N, Hentschel U (2008) Molecular microbial diversity survey of sponge reproductive stages and mechanistic insights into vertical transmission of microbial symbionts. Appl Environ Microbiol 74:7694–7708
28. Caporaso JG, Lauber CL, Walters WA, Berg-Lyons D, Lozupone CA, Turnbaugh PJ, Fierer N, Knight R (2011) Global patterns of 16S rRNA diversity at a depth of millions of sequences per sample. Proc Natl Acad Sci 108:4516–4522
29. Schloss PD, Westcott SL, Ryabin T, Hall JR, Hartmann M, Hollister EB, Lesniewski RA, Oakley BB, Parks DH, Robinson CJ, Sahl JW, Stres B, Thallinger GG, Van Horn DJ, Weber CF (2009) Introducing mothur: open-source, platform-independent, community-supported software for describing and comparing microbial communities. Appl Environ Microbiol 75:7537–7541
30. Huse SM, Welch DM, Morrison HG, Sogin ML (2010) Ironing out the wrinkles in the rare biosphere through improved OTU clustering. Environ Microbiol 12:1889–1898
31. Narum SR (2006) Beyond Bonferroni: less conservative analyses for conservation genetics. Conserv Genet 7:783–787
32. White JR, Nagarajan N, Pop M (2009) Statistical methods for detecting differentially abundant features in clinical metagenomic samples. PLoS Comput Biol 5:e1000352
33. Altschul SF, Gish W, Miller W, Myers EW, Lipman DJ (1990) Basic local alignment search tool. J Mol Biol 215:403–410
34. López-Legentil S, Erwin PM, Pawlik JR, Song B (2010) Effects of sponge bleaching on ammonia-oxidizing Archaea: distribution and relative expression of ammonia monooxygenase genes associated with the barrel sponge *Xestospongia muta*. Microb Ecol 60:561–571
35. Gao Z-M, Wang Y, Tian R-M, Lee OO, Wong YH, Batang ZB, Al-Suwailem A, Lafi FF, Bajic VB, Qian P-Y (2015) Pyrosequencing revealed shifts of prokaryotic communities between healthy and disease-like tissues of the Red Sea sponge *Crella cyathophora*. Peer J 3:e890. https://doi.org/10.7717/peerj.890
36. Brochier-Armanet C, Boussau B, Gribaldo S, Forterre P (2008) Mesophilic *Crenarchaeota*: proposal for a third archaeal phylum, the *Thaumarchaeota*. Nat Rev Microbiol 6:245–252
37. Pester M, Schleper C, Wagner M (2011) The *Thaumarchaeota*: an emerging view of their phylogeny and ecophysiology. Curr Opin Microbiol 4:300–306
38. Radax R, Hoffmann F, Rapp HT, Leininger S, Schleper C (2012) Ammonia-oxidizing Archaea as main drivers of nitrification in cold-water sponges. Environ Microbiol 14:909–923
39. Zhang F, Pita L, Erwin PM, Abaid S, López-Legentil S, Hill RT (2014) Symbiotic archaea in marine sponges show stability and host specificity in community structure and ammonia oxidation functionality. FEMS Microbiol Ecol 90:699–707
40. Sunagawa S, DeSantis TZ, Piceno YM, Brodie EL, DeSalvo MK, Voolstra CR, Weil E, Andersen GL, Medina M (2009) Bacterial diversity and white plague disease-associated community changes in the Caribbean coral *Montastraea faveolata*. ISME J 3:512–521
41. Witt V, Wild C, Anthony KR, Diaz-Pulido G, Uthicke S (2011) Effects of ocean acidification on microbial community composition of, and oxygen fluxes through, biofilms from the great barrier reef. Environ Microbiol 13:2976–2989
42. Olson JB, Gao X (2013) Characterizing the bacterial associates of three Caribbean sponges along a gradient from shallow to mesophotic depths. FEMS Microbiol Ecol 85:74–84